Journal of Biomolecular NMR **30:** 389–395, 2004.

Homonuclear chemical shift correlation in rotating solids via RN_n^v symmetry-based adiabatic RF pulse schemes

Kerstin Riedel, Jörg Leppert, Sabine Häfner, Oliver Ohlenschläger, Matthias Görlach & Ramadurai Ramachandran*

Abteilung Molekulare Biophysik/NMR-Spektroskopie, Institut für Molekulare Biotechnologie, 07745 Jena, Germany

Received 7 June 2004; Accepted 16 September 2004

Key words: adiabatic pulse, chemical shift correlation, MAS, solid state NMR

Abstract

The efficacy of RN_n^v symmetry-based adiabatic Zero-Quantum (ZQ) dipolar recoupling schemes for obtaining chemical shift correlation data at moderate magic angle spinning frequencies has been evaluated. RN_n^v sequences generally employ basic inversion elements that correspond to a net 180° rotation about the rotating frame x-axis. It is shown here via numerical simulations and experimental measurements that it is also possible to achieve efficient ZQ dipolar recoupling via RN_n^v schemes employing adiabatic pulses. Such an approach was successfully used for obtaining ^{13}C chemical shift correlation spectra of a uniformly labelled sample of $(CUG)_{97}$ – a triplet repeat expansion RNA that has been implicated in the neuromuscular disease myotonic dystrophy. An analysis of the ^{13}C sugar carbon chemical shifts suggests, in agreement with our recent ^{15}N MAS-NMR studies, that this RNA adopts an A-helical conformation.

Introduction

MAS solid state NMR is emerging as an important tool for structural studies of systems that are not easily amenable via solution state NMR. In the investigation of isotopically labelled biological molecules chemical shift correlation experiments are commonly employed e.g., for assignment of NMR resonances and for obtaining structural constraints such as internuclear distances. Although weak dipolar couplings between low γ nuclei are averaged out under MAS, efficient techniques have been developed in recent years to recouple weak homo- and heteronuclear dipolar interactions (Bennett et al., 1994; Griffin, 1998; Dusold and Sebald, 2000). It has been shown that these recoupled dipolar interactions can be conveniently used to generate chemical shift correlation data under magic angle spinning conditions. Making use of the rotational properties of the nuclear spin interactions and the application of rotor-synchronised RF pulse sequences, a symmetry-based approach has been proposed by Levitt and co-workers for effecting the evolution of the spins under the desired average Hamiltonian of interest under magic angle spinning conditions (Carravetta et al., 2000; Brinkmann and Levitt, 2001; Levitt, 2002). Two class of symmetry-based pulse sequences, denoted as CN_n^v and RN_n^v, have been introduced till date. The CN_n^v class of RF pulse schemes involves the repeated application of a basic element 'C' corresponding to an RF cycle with unity propagator $U_{RF}(\tau_C) = \pm 1$. N such cycles are applied over n rotor periods τ_r. Successive C elements are incremented in phase by $v2\pi/N$ and typically the complete CN_n^v sequence is repeated many times. In

*To whom the correspondence should be addressed. E-mail: raman@imb-jena.de

the RN_n^v scheme, defined also by the three integer symmetry numbers N, n and v, the critical basic component is an inversion element 'R'. A pair of appropriately phase-shifted pulses is derived from this basic element to form a RF pulse sandwich '**R**' corresponding to a propagator $U_{RF} = \exp(-i4\phi I_z)$, representing a net rotation of 4ϕ about the z-axis where $\phi = v\pi/N$. The pulse sandwich '**R**' is repeated $N/2$ times over n rotor periods so as to form an RF cycle with unity propagator $U_{RF}(\tau_C) = \pm 1$. The performance of the symmetry-based schemes in general critically depends on the choice of the basic element. N, n and v are all integers and appropriate values for these are chosen, via the selection rule for CN_n^v and RN_n^v symmetry, to generate the desired average Hamiltonian with high efficiency. Symmetry-based sequences have found extensive usage in the study of biological systems. For example, RN_n^v and CN_n^v sequences have recently been reported for generating ^{13}C chemical shift correlation data at high MAS frequencies (Brinkmann et al., 2002; Hardy et al., 2003).

All RN_n^v symmetry-based pulse sequences developed till date make use of R elements that correspond to a net rotation of 180° around the rotating frame x-axis. However, it is seen from the studies reported here that it is not necessary that the R element should satisfy such a requirement. For example, the propagator for an adiabatic inversion pulse (Baum et al., 1985; Kupce and Freeman, 1995a, b, 1996; Tannus and Garwood, 1996; Hwang et al., 1998), that acts properly only on the z component and not on the transverse magnetisation components, does not correspond to a 180°_x pulse. However, it is possible to implement efficient RN_n^v symmetry-based pulse sequences employing adiabatic pulses and this can be rationalised as follows. Suppose the Euler angles (α_n, β_n, γ_n) represent the *net* rotation of the spins induced by an adiabatic inversion pulse with x phase, i.e., $U_{RF}(net) = \exp(-i\alpha_n I_z)\exp(-i\beta_n I_y)\exp(-i\gamma_n I_z)$. As adiabatic inversion pulses induce good inversion of z magnetisation components, the Euler angle β_n has to have a value of 180° while the other two Euler angles can take any value depending on the pulse characteristics. As the Euler angles for adiabatic pulses with phase $+\phi$ and $-\phi$ respectively are $\{\alpha_n+\phi, \beta_n, \gamma_n-\phi\}$ and $\{\alpha_n-\phi, \beta_n, \gamma_n+\phi\}$, the net propagator of $\{R_\phi R_{-\phi}\}$ corresponds to $\exp(-i4\phi I_z)$. Just as U_{RF} (*net*) can be represented in terms of the Euler angles (α_n, β_n, γ_n), it is also possible to represent the propagator $U_{RF}(t, t_0)$, corresponding to the time-dependent rotation of spins during the application of an adiabatic pulse, in terms of the time-dependent Euler angles ($\alpha(t)$, $\beta(t)$, $\gamma(t)$) with t_0 and t representing the starting initial and final end points of the pulse (Zhou et al., 1994). Considering once again adiabatic pulses with phases zero, $+\phi$ and $-\phi$ it is expected that $\beta(t)$ for all three pulses will remain the same and the γ Euler angle difference between the phase shifted pulses will be just 2ϕ. As a result, in any RN_n^v symmetry-based adiabatic pulse scheme employing the RF pulse sandwich $\mathbf{R} = \{R_\phi R_{-\phi}\}$, the Euler angles representing the propagator for the applied RF fields are expected to follow the time-symmetry relationships required by RN_n^v schemes (Carravetta et al., 2000; Brinkmann and Levitt, 2001; Levitt, 2002). With $\phi = v\pi/N$, repeating $N/2$ times this sandwich **R** over n rotor periods would lead to a unity RF propagator as required in the Average Hamiltonian theory based RN_n^v pulse sequence construction. Since the RF pulse sandwich $\mathbf{R} = \{R_\phi R_{-\phi}\}$ formed with adiabatic inversion pulses satisfies the necessary requirements imposed by RN_n^v symmetry-based pulse schemes, it should also be feasible to design efficient RN_n^v symmetry-based pulse sequences employing adiabatic pulses. The numerical simulations and experimental measurements presented here confirm these expectations. Although not mentioned, the possibilities for RN_n^v symmetry-based adiabatic pulse schemes can be inferred from the recent adiabatic TOBSY study of Hardy et al. (2003). We have explored here for the first time RN_n^v symmetry-based adiabatic pulse sequences in the context of ZQ dipolar recoupling at moderate MAS frequencies. We employed RN_n^v symmetry-based adiabatic RF pulse scheme for obtaining ^{13}C correlation data of a 100 kDa RNA in the solid state. The system studied is a triplet expansion repeat RNA composed of 97 CUG triplets, or $(CUG)_{97}$. CUG repeats > 50 have been implicated in the neuromuscular disease myotonic dystrophy type 1 (DM1; Nykamp and Swanson, 2004; Ranum and Day, 2004). Biochemical and electronmicroscopy studies suggested that these repeats fold into large and stable double-stranded (ds) RNA hairpins (Napierala and Krzyzosiak, 1997; Michalowski et al., 1999) which bind and

sequester the muscleblind (MBNL) proteins (Miller et al., 2000; Kanadia et al., 2003). Sequestration and loss of MBNL function leads to misregulation of alternative pre-mRNA splicing of a number of gene transcripts. For example, the major skeletal muscle chloride channel CIC1 is mis-spliced in both human DM1 and mouse Mbnl1Δ^{E3}/Δ^{E3} knockout muscle leading to loss of normal chloride conductance and muscle hyperexcitability (myotonia) (Charlet et al., 2002; Mankodi et al., 2002) and Mbnl1 knockout mice show abnormalities that are characteristic of DM disease (Kanadia et al., 2003). Recently we have provided direct evidence that this RNA indeed adopts a double-stranded conformation (Leppert et al., 2004a).

Numerical and experimental procedures

Numerical simulations were carried out using the SIMPSON program (Bak et al., 2000) considering two spin-1/2 nuclei and a Zeeman field strength of 11.7 T. The efficacy of symmetry-based adiabatic pulse schemes were assessed by monitoring the z magnetisation transferred to the second spin ($^{13}C'/^{13}C^{\beta}$) as a function of the mixing time, starting with z magnetisation on spin 1 ($^{13}C^{\alpha}$). Unless mentioned otherwise, ^{13}C scalar coupling, chemical shift and dipolar tensor parameters of alanine ($C^{\alpha} \rightarrow C^{\beta}$) and glycine ($C^{\alpha} \rightarrow C'$) were employed in these simulations (Brinkmann et al., 2002). The 'cagauss' adiabatic pulses (Kupce and Freeman, 1996), as implemented in the Varian pulse-shaping software 'Pbox', and tanh/tan adiabatic pulses (Hwang et al., 1998) were employed with durations, power levels and phasing scheme as given in the figure captions. All tanh/tan pulses used in this work had a pulse bandwidth and pulse length product (Hwang et al., 1998) value of 60. The $\{^{15}N, ^{13}C\}$ labelled hydrated $(CUG)_{97}$ RNA sample was prepared using doubly labelled NTPs exactly as described earlier (Leppert et al., 2004a). NMR experiments were carried out at approximately −15 °C on a 500 MHz wide-bore Varian ^{UNITY}*INOVA* solid state NMR spectrometer equipped with a 5 mm DOTY supersonic triple resonance probe and a waveform generator for pulse shaping. The RF pulse sequence employed for generating chemical shift correlation spectra, via adiabatic symmetry-based ZQ dipolar recoupling mixing scheme, was similar to that we have used in our recent studies (Leppert et al., 2003, 2004a, b). Cross-polarisation under Hartmann–Hahn matching conditions was employed and all spectra, unless mentioned otherwise, were collected under high power ^{1}H decoupling (~90 kHz). Typical ^{1}H, ^{15}N and ^{13}C 90° pulse widths were 2.8, 7.5 and 5.5 μs, respectively. Other details are given in the figure captions. ZQ dipolar recoupling was carried out with either the $R6_6^2R6_6^{-2}$ or the $SR6_6^2$ supercycled sequence reported by Brinkmann et al. (2002).

Results and discussion

Brinkmann et al. (2002) have demonstrated recently the effectiveness of RN_n^{ν} schemes for ZQ recoupling at high MAS frequencies. It is seen from their studies that the efficacy of ZQ dipolar recoupling employing the composite pulse inversion element R $[90_{180}270_0]$ deteriorates at moderate to low spinning frequencies and at high fields. Although studies at very high spinning speeds are attractive, with many biological systems it is difficult to use very fast spinning speeds, e.g., to avoid sample dehydration. Experiments at moderate spinning speeds are also often sufficient in situations where spinning sideband intensities are not significant. With these considerations in mind, we have assessed the performance of RN_n^{ν} ZQ recoupling schemes employing an adiabatic inversion element R. The simulations were carried out at a few representative spinning speeds and for a comparison the ZQ recoupling performance seen with the composite pulse inversion element R $[90_{180}270_0]$ (Brinkmann et al., 2002) is also indicated. It is worth mentioning here that while the recoupling RF field strength needed with the composite pulse R element is related to the spinning speed (Brinkmann et al., 2002), the RF field strength required with adiabatic pulses is dependent only on the pulse characteristics. In Figure 1, we show the ZQ recoupling characteristics seen at spinning speeds of 7000 Hz (a), 10000 Hz (b) and 15000 Hz (c) with the schemes $SR6_6^2$ (a) and $R6_6^2R6_6^{-2}$ (b) and (c), respectively. The plots shown in Figure 1a were generated using a dipolar coupling strengths in the range of 50–250 Hz and neglecting scalar couplings. These

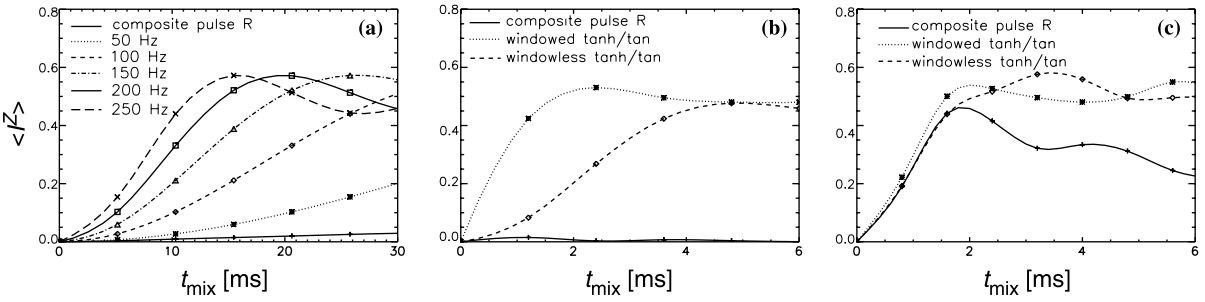

Figure 1. Magnitude of the transferred magnetisation on spin 2 ($^{13}C^{\beta}$) (normalised to the maximum transferable signal), starting with longitudinal magnetisation on spin 1 ($^{13}C^{\alpha}$) at zero mixing time. The plots at the spinning speed of 7000 Hz (a) were generated as a function of the dipolar coupling strength indicated, neglecting the scalar coupling between the nuclei, employing the ZQ dipolar recoupling scheme $SR6_6^2$ with 'cagauss' adiabatic pulses (142 μs, 25.0 kHz γH_1, 40 kHz sweep). The sampled data points were interpolated to provide visual clarity. For comparison, a representative plot generated at a dipolar coupling strength of 100 Hz and using the composite pulse *R* element [$90_{180}270_0$] (Brinkmann et al., 2002) with the $SR6_6^2$ scheme is also given. An isotropic chemical shift difference of ± 5000 Hz was employed in these simulations. The plots at the spinning speed of 10000 Hz (b) and 15000 Hz (c) were generated with the $R6_6^2R6_6^{-2}$ scheme considering the $C^{\alpha} \rightarrow C'$ and $C^{\alpha} \rightarrow C^{\beta}$ transfers, respectively, and applying one bond dipolar and scalar coupling values. (b) Shows the plots obtained with windowless and windowed (see text) tanh/tan adiabatic pulse *R* elements of 100 μs (30.0 kHz γH_1) and 40 μs (40.0 kHz γH_1) durations and with an isotropic chemical shift difference of ± 8000 Hz. (c) Shows the plots obtained with windowless and windowed tanh/tan adiabatic pulse *R* elements of 66.66 μs (40.0 kHz γH_1) and 40 μs (40.0 kHz γH_1) durations and using an isotropic chemical shift difference of ± 6000 Hz. For comparison, (b) and (c) also show the plots obtained with windowless composite pulse *R* element [$90_{180}270_0$] employing the $R6_6^2R6_6^{-2}$ scheme.

plots show that the initial rate of transfer of magnetisation from spin 1 to spin 2 is highly sensitive to the dipolar coupling strength and hence to internuclear distances. The ZQ recoupling performance with the composite pulse, as seen from one of the representative plots shown, is not satisfactory. However, the good performance seen with adiabatic pulses suggests that adiabatic RN_n^{ν} ZQ recoupling schemes can also be successfully employed at low spinning speeds for obtaining reliable estimates of internuclear distances.

When dealing with large internuclear distances and hence weak dipolar couplings a large dipolar mixing period is required to achieve sufficient transfer of polarisation from one spin to another. Under these circumstances it becomes possible to use efficient supercycles for improving the pulse sequence performance characteristics. However, at moderate spinning speeds and when only short mixing times are required, as in ^{13}C chemical shift correlation studies of uniformly labelled samples, it is not advantageous to use supercycles. Hence, the simulations shown in Figures 1b and 1c, depicting respectively the efficacy of $C^{\alpha} \rightarrow C'$ and $C^{\alpha} \rightarrow C^{\beta}$ transfers, were carried out with the simpler pulse scheme $R6_6^2R6_6^{-2}$. Other relevant parameters are given in the figure captions. The $R6_6^2R6_6^{-2}$ scheme essentially involves the application of one *R* element per rotor period. In the conventional approach the duration of the *R* element is chosen such that it occupies the entire rotor period. For example, at a spinning speed of 10000 Hz, it is necessary to use an adiabatic pulse of 100 μs duration. Although in the context of minimising the recoupling RF field strength it is advantageous to use adiabatic pulses with large durations, it is seen from numerical simulations that improved broadband ZQ recoupling at moderate spinning frequencies can be achieved in general by employing windowed *R* elements (Levitt, 2002; Eden, 2003) in the RN_n^{ν} schemes. The windowed *R* element used in our study essentially involves the following sandwich of delays and pulse: $\{\tau_w - P - \tau_w\}$. The total duration of the windowed *R* element equals the rotor period and *P* is the inversion element. The simulations with adiabatic pulses were carried out with both the windowless and windowed *R* elements and from the plots shown in Figures 1b and 1c it is clearly seen that adiabatic inversion pulses can be successfully employed in RN_n^{ν} schemes. The ZQ recoupling performance observed with the RN_n^{ν} scheme is in general similar to what is observed in our recent RFDR studies with adiabatic pulses (Leppert et al., 2003, 2004a, b).

Employing $R6_6^2R6_6^{-2}$ symmetry-based adiabatic ZQ recoupling scheme we have obtained the dipolar ^{13}C chemical shift correlation spectrum of the 100 kDa RNA $(CUG)_{97}$. Figure 2

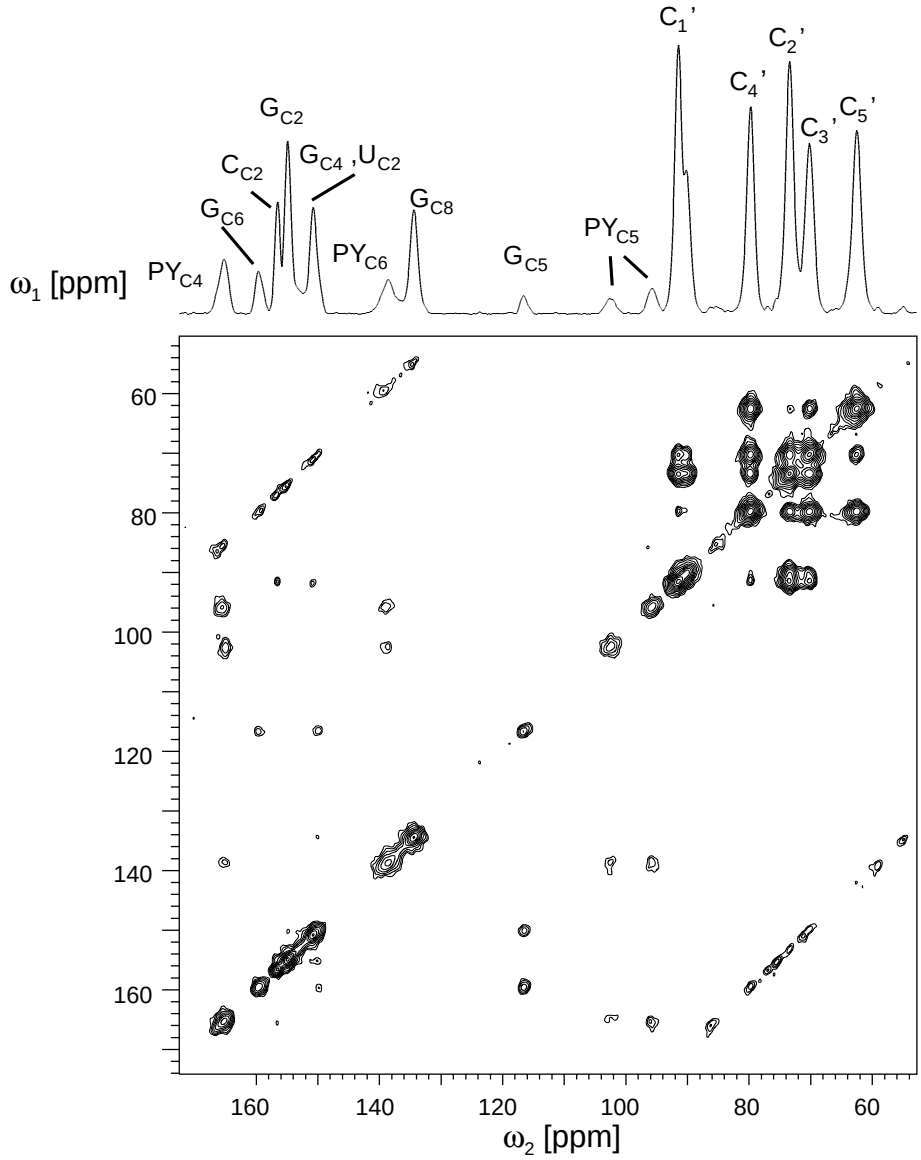

Figure 2. Experimental ^{13}C ZQ correlation spectrum (zoomed plot) of hydrated RNA obtained at a spinning speed of 10000 Hz employing adiabatic symmetry-based scheme $R6_6^2R6_6^{-2}$, a recycle time of 2 s, 16 scans per t_1 increment and with ω_1 spectral width of 25000 Hz. This spectrum was collected with windowed tanh/tan adiabatic inversion pulses of 40 μs duration, $\omega_1(\max)/2\pi$ of $\sim$37 kHz and keeping the RF carrier at the center of the spectral range. Chemical shifts are referenced with respect to external adamantane ($\delta_{CH} = 29.5$ ppm with respect to TMS).

shows the correlation spectrum generated at a spinning speed of 10000 Hz and at a representative mixing time of 2.4 ms. As with earlier studies carried out on mono-nucleotides (Sun et al., 1997; Kiihne et al., 1999), the spectrum shown in Figure 2 clearly reveals all the expected correlation peaks. The assignments on the spectral projection shown are based on data collected at different mixing times and on isotropic chemical shifts typically observed in solution state NMR studies of RNAs (Wijmenga and Van Buuren, 1998). Many of the carbon resonances are not well resolved in the 2D correlation spectrum shown. Within the resolution of the spectrum acquired ($\sim$0.4 ppm), all C2′, C3′, C4′ and C5′ sugar carbon atoms of the three nucleotides

exhibit degenerate resonances at 73.1, 70.0, 79.5 and 62.3 ppm. Two distinct C1′ resonances at 91.2 and 90.8 ppm, possibly arising from the pyrimidines (U & C) and purine (G) respectively, are seen. Following a statistical analysis of the dependence of ^{13}C NMR chemical shifts on the conformations of RNA nucleosides and nucleotides reported by Ebrahimi et al. (2001), the sugar carbon chemical shifts of the $(CUG)_{97}$ RNA were analysed in structural terms. This analysis correlates data for the sugar pucker, the exocyclic angle γ and the glycosidic angle χ with the carbon chemical shifts of the sugar moiety. It was observed that the canonical coordinates for standard conformations like N/*gg*/*anti*, N/*gt*/*anti* as well as S/*gg*/*syn* and S/*gg*/ *anti* group in distinct areas of this plot. Figure 3 shows the canonical coordinates for $(CUG)_{97}$ RNA (−5.32, −16.42) calculated with the formulae:

$$can1 = 0.179 * \delta_{C1'} - 0.225 * \delta_{C4'} - 0.0585 * \delta_{C5'} \text{ and}$$

$$can2 = -0.0605 * (\delta_{C2'} + \delta_{C3'}) - 0.0556 * \delta_{C4'} - 0.0524 * \delta_{C5'}.$$

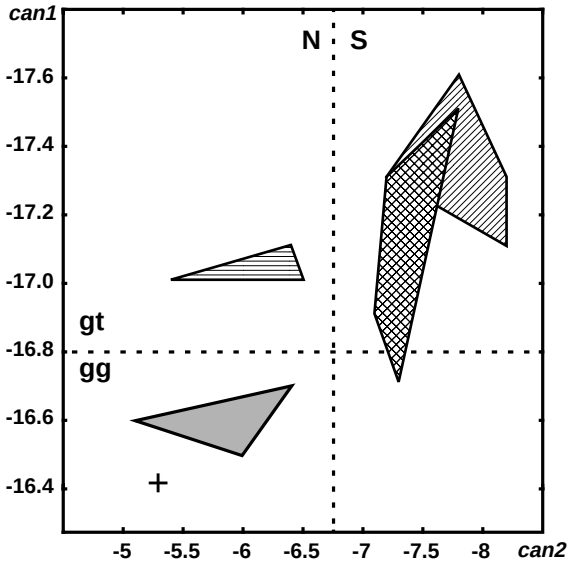

Figure 3. Canonical coordinates plot (adapted from Ebrahimi et al., 2001). The hatched, criss-crossed, lined and dotted regions correspond to S/gg/anti, S/gg/syn, N/gt/ anti and N/gg/ anti conformations, respectively. The cross indicates the coordinate position for $(CUG)_{97}$. The vertical and horizontal lines separate the C3′-endo (A-form RNA) and C2′-endo as well as the *gt* and *gg* region, respectively.

The coordinate for $(CUG)_{97}$ RNA projected onto this plot falls in the region with N-type sugar pucker, a *gauche–gauche* conformation for the backbone torsion angle γ and an *anti* conformation of the glycosidic angle χ. This result suggests an A-form helical RNA conformation for $(CUG)_{97}$, in agreement with our recent ^{15}N MAS-NMR study (Leppert et al., 2004a) while a 'toblerone'-like structure as proposed in the CD study for $(CUG)_5$ repeats (Pinheiro et al., 2002) involving e.g., *syn*-G conformations differs from the results obtained in this study.

In conclusion, the results presented here show that it is possible to implement RN^{ν}_{n} symmetry-based pulse schemes with adiabatic inversion pulses. While Brinkmann et al. (2002) have recently demonstrated homonuclear ZQ dipolar recoupling via RN^{ν}_{n} symmetry-based schemes at very high MAS frequencies, we have extended the applicability of this approach to the lower MAS frequency regime. The quality of the ^{13}C chemical shift correlation spectrum of the RNA presented here demonstrates clearly the potential of MAS NMR for the study of large RNA systems, considering the difficulties of solution state NMR studies of large RNAs. However, the limited spectral resolution seen in the 2D ^{13}C correlation spectrum suggests that it will be necessary to employ ^{15}N-edited experiments in the structural studies of RNAs in the solid state. Such heteronuclear experiments to obtain site-specific resonance assignments have been carried out for $(CUG)_{97}$ and the results from these investigations will be reported elsewhere.

References

Bak, M., Rasmussen, J.T. and Nielsen, N.C. (2000) *J. Magn. Reson.*, **147**, 296–330.

Baum, J., Tycko, R. and Pines, A. (1985) *Phys. Rev. A*, **32**, 3435–3447.

Bennett, A.E., Griffin, R.G. and Vega, S. (1994) *NMR Basic Principles and Progress*, Vol. 33, Springer Verlag, Berlin, pp. 1–77.

Brinkmann, A. and Levitt, M.H. (2001) *J. Chem. Phys.*, **115**, 357–384.

Brinkmann, A., Schmedt auf der Günne, J. and Levitt, M.H. (2002) *J. Magn. Reson.*, **156**, 79–96.

Carravetta, M., Eden, M., Zhao, X., Brinkmann, A. and Levitt, M.H. (2000) *Chem. Phys. Lett.*, **321**, 205–215.

Charlet, B.N., Savkur, R.S., Singh, G., Philips, A.V., Grice, E.A. and Cooper, T.A. (2002) *Mol. Cell*, **10**, 45–53.

Dusold, S. and Sebald, A. (2000) *Annu. Rep. NMR Spectrosc.*, **41**, 185–264.

Ebrahimi, M., Rossi, P., Rogers, C. and Harbison, G.S. (2001) *J. Magn. Reson.*, **150**, 1–9.
Eden, M. (2003) *Chem. Phys. Lett.*, **378**, 55–64.
Griffin, R.G. (1998) *Nat. Struct. Biol.*, **5**, 508–512.
Hardy, E.H., Detken, A. and Meier, B.H (2003) *J. Magn. Reson.*, **165**, 208–218.
Hwang, T., van Zijl, P.C.M. and Garwood, M. (1998) *J. Magn. Reson.*, **133**, 200–203.
Kanadia, R.N., Johnstone, K.A., Mankodi, A., Lungu, C., Thornton, C.A., Esson, D., Timmers, A.M., Hauswirth, W.W. and Swanson, M.S. (2003) *Science*, **302**, 1978–1980.
Kiihne, S.R., Geahigan, K.B., Oyler, N.A., Zebroski, H., Mehta, M.A. and Drobny, G.P. (1999) *J. Phys. Chem. A*, **103**, 3890–3903.
Kupce, J. and Freeman, R. (1995a) *J. Magn. Reson. A*, **115**, 273–276.
Kupce, J. and Freeman, R. (1995b) *J. Magn. Reson. A*, **117**, 246–256.
Kupce, J. and Freeman, R. (1996) *J. Magn. Reson. A*, **118**, 299–303.
Leppert, J., Heise, B., Ohlenschläger, O., Görlach, M. and Ramachandran, R. (2003) *J. Biomol. NMR*, **26**, 13–24.
Leppert, J., Urbinati, C.R., Häfner, S., Ohlenschläger, O., Swanson, M.S., Görlach, M. and Ramachandran, R. (2004a) *Nucl. Acids Res.*, **3**, 1177–1183.
Leppert, J., Ohlenschläger, O., Görlach, M. and Ramachandran, R. (2004b) *J. Biomol. NMR*, **28**, 229–233.
Levitt, M.H. (2002) In *Encyclopedia of NMR*, Vol. 9, pp. 165–196.
Mankodi, A., Takahashi, M.P., Jiang, H., Beck, C.L., Bowers, W.J., Moxley, R.T., Cannon, S.C. and Thornton, C.A. (2002) *Mol. Cell*, **10**, 35–44.
Michalowski, S., Miller, J.W., Urbinati, C.R., Paliouras, M., Swanson, M.S. and Griffith, J. (1999) *Nucl. Acids Res.*, **27**, 3534–3542.
Miller, J.W., Urbinati, C.R., Teng-Umnuay, P., Stenberg, M.G., Byrne, B.J., Thornton, C.A. and Swanson, M.S. (2000) *EMBO J.,* **19**, 4439–4448.
Napierala, M. and Krzyzosiak, W.J. (1997) *J. Biol. Chem.*, **272**, 31079–31085.
Nykamp, K.R. and Swanson, M.S. (2004) *Prog. Mol. Subcell. Biol.,* **35**, 57–77.
Pinheiro, P., Scarlett, G., Rodger, A., Rodger, P.M., Murray, A., Brown, T., Newbury, S.F. and McClellan, J.A. (2002) *J. Biol. Chem.* **277**, 35183–35190.
Ranum, L.P.W. and Day, J.W. (2004) *Am. J. Hum. Genet.* **74**, 793–804.
Sun, B.-Q., Rienstra, C.M., Costa, P.R., Willamson, J.R. and Griffin, R.G. (1997) *J. Am. Chem. Soc.*, **119**, 8540–8546.
Tannus, A. and Garwood, M. (1996) *J. Magn. Reson. A,* **120**, 133–137.
Wijmenga, S.S. and van Buuren, B.N.M. (1998) *Prog. Nucl. Magn. Reson. Spectrosc.*, **32**, 287–387.
Zhou, J., Ye, C. and Sanctuary, B.C. (1994) *J. Chem. Phys.*, **101**, 6424–6429.